IRAQI JOURNAL OF MATERIALS
Volume (5) Issue (3) July-September 2026, pp. 121-126
Published and Sponsored by American Quality for Scientific Publishing, Inc. (AQSP)

Tailoring Interface-Induced Chirality in Synthetic Antiferromagnets for Next-Generation Spintronics through Strategic Heavy Metal Layer Optimization

Fadel H. Dayeh[1], Ala A. Manzoor[2], Jafaar O. Radi[3*]

[1] *Department of Physics, College of Science, Misan University, Al Amarah, IRAQ*
[2] *Department of Physics, College of Science, Thi Qar University, Nasiriya, IRAQ*
[3] *Department of Physics, College of Science, Al Qadisiyah University, Diwaniyah, IRAQ*
[*] *Corresponding author email: jaafar.odeh2017@gmail.com*

Abstract
This study explores the possibility of designing induced chirality at the interfaces in the synthetic antiferromagnetics (SAFs) throughout enhancing the heavy metal layer in the multilayer structures based on these materials for the applications of the next generation spintronics. This study considers the spin-orbit interaction (SOI) and Dzyaloshinskii-Moriya Interaction (DMI) to achieve control of spin current flow direction and spinal structures such as skyrmions. Results showed that platinum can produce higher DMI energy density of 1.3 mJ/m^2 at layer thickness of 35 µm when compared to tantalum and tungsten. The optimized model of the multilayer structure showed velocities up to 10^3 m/s at low threshold current density of $1.2x10^{11}$ A/m^2 with superiority over the standard model. These models allow the development of ultrafast and low-energy magnetic random-access memories (MRAM) for neural computers and new generations of effective spintronics.

***Keywords*:** Spintronics; Dzyaloshinskii-Moriya Interaction (DMI); Magnetic chirality; Synthetic Antiferromagnets
Received: February 2026; **Revised:** April 2026; **Accepted:** May 2026; **Published:** July 2026

1. Introduction

Spintronics have witnessed radical transformations during the last few decades throughout exceeding the conventional dependence on electron charge to include the feature of spin momentum. The ability to control and process spin currents represent the cornerstone in modern spintronics such as magnetic random-access memories (MRAMs) and spin-torque oscillators [1-3]. However, there some major challenges against the progress in this discipline like the need for high-density currents to invert the magnetic polarity. This limits the energy efficiency and extension capability. Here, the concept of spin-orbit interaction (SOI) is seen as a promising solution as it allows the generation of pure and active spin currents via effects like spin Hall effect (SHE) and Edelstein-Rashba effect [4,5]. Inside the core of this revolution, magnetic chirality is defined as an engineering property determining the direction of spin-orbit torque in spiral or vortices-like magnetic structures. The accurate control of chirality – especially at the interfaces of the materials – opens the door for a new generation of ultrafast energy-saving devices [6].

The SOI originates from the relative connection between spin torque of electron and its orbital momentum. In materials of high atomic number (heavy metals like platinum, tantalum, and tungsten), this interaction becomes very strong to induce two main phenomena [7]. As the first phenomenon, in presence of an electric current, the SOI leads to deflect electrons of reverse spin torques towards two opposite and perpendicular directions and this generates transverse spin current. This mechanism is effective in generating spin-orbit torque (SOT), which is able to invert the magnetic polarity in an adjacent layer [8]. The second phenomenon is the Dzyaloshinskii-Moriya Interaction (DMI), which is the key to understand the chirality. The DMI occurs at the interfaces between heavy metal layer and ferromagnetic layer due to strong SOI of the heavy metal [9]. Different from the conventional magnetic exchange (Heisenberg exchange) that prefers parallel of anti-parallel components of spin momenta, DMI prefers the normal or perpendicular components leading to form chiral spin textures, such as Néel field walls or spiral magnetic zone (skyrmions) [10]. The sign of DMI (positive or negative) determines the spiral direction (or chirality) of these structures, and hence, the control of DMI strength allows the design of chirality [11,12].

IRAQI JOURNAL OF MATERIALS
Volume (5) Issue (3) July-September 2026, pp. 121-126
Published and Sponsored by American Quality for Scientific Publishing, Inc. (AQSP)

Despite that the individual ferromagnetic layers are well studied, they suffer the problem of magnetic stray fields those limit the storage density and maintain the stability of chirality structures. Therefore, the synthetic antiferromagnets (SAFs) are employed [13-15]. The SAF is usually composed of two ferromagnetic layers or thin films separated by a thin layer of nonmagnetic metal (such as ruthenium or iridium) known as “spacer”. The antiferromagnetic exchange coupling through the spacer parallel to the spin momenta of both SAFs layers (i.e., opposite) [16]. The SAFs show crucial features such as stray-field-free, high resonance frequencies, and enhanced thermal stability. Due to the opposite momenta, their stray fields totally cancel each other, which allow high concentration of magnets without interference [17]. The SAFs show ferromagnetic resonance (FMR) within the high frequency range (from GHz to THz) that make then ideal candidates for ultrafast applications. The layer thicknesses and antiparallel exchange can be adjusted to achieve high stability against thermal fluctuations [18].

The pivotal question to be answered in this work is how the SAFs advantages can be invested together with the interface-induced chirality?

In a conventional SAF structure composed of lower layer of heavy metal (HM), first ferromagnet layer (FM1), nonmagnetic spacer, second ferromagnet layer (FM2), upper layer (cap) of heavy metal (HM), the heavy metal layers have crucial dual role. They generate spin currents via SHE as the electric current passing through the lower HM layer results in a spin current flowing to the FM1 layer due to SHE and imposing spin-orbit torque (SOT), which is the usual strategy to invert the magnetic polarity. They also form a DMI at the interface HM/FM, which is the most innovative aspect [19-21]. The strength and signal of DMI induced at the interface HM/FM1 differ from those induced at the interface HM/FM2. This is reasonably dependent on the type of the metal (Pt, Ta, W, Ir, Au, etc.) as well as its thickness, crystallinity and surface condition [22].

The ability to design chirality in the SAFs throughout modifying the heavy metal layer may present new practical solutions. The designed chirality can be to facilitate the skyrmions at ultrahigh velocities and very low currents in the super-efficient SOT-MRAMs. This allows data transfer at energies reasonably lower than the current technologies [23-25]. Different chirality structures can represent logic states (0 and 1) and electric current can “write” these states throughout the chirality core. This principle is the base of the reconfigurable spin logic [26]. The chirality affects the resonance frequency of the momentum structures in the SAFs that allows to fabricate spin-torque oscillators with adjustable frequency range considering the heavy metal design [27]. The spiral dynamics of skyrmions simulate the behavior of neural cells and the SAFs based on designed chirality can be used to construct spiral neural networks for unconventional neuromorphic computing [28,29].

In this study, the combination of the spin-orbit interaction (SOI), Dzyaloshinskii-Moriya Interaction (DMI) and synthetic antiferromagnets (SAFs) is studied to understand that it can provide a rich platform for modern physics and revolutionary applications. Such platform can be mainly controlled by the heavy metal layer acting as a source for the spin currents and an intermediate for the induced magnetic chirality. By modifying materials, thickness and morphology of these layers, the interface chirality can be accurately designed to overcome the restrictions of the conventional systems. The aim of this study is to present experimental results to confirm the feasibility of the proposed method as well as to determine the optimum pathways to achieve controlled chirality in the SAFs. This may pave the road to a new generation of high-efficient, fast and flexible spintronics.

2. Experimental Part

The magnetron sputtering system is provided with 6 cathode holders to allow the serial deposition of different layers under vacuum. The base pressure was 10^{-8} torr in order to minimize the contamination with residual gases, such as oxygen and water vapor, which negatively affect the interfaces. The reactive gas was highly-pure (99.99%) argon at pressure of 0.002 torr. More details on this system can be found elsewhere [30-33].

Silicon wafers of 300 μm thickness and (111) orientation were used as the substrates on which the multilayer structures were grown. The silicon wafer is coated with a thin SiO_2 layer on its top surface to prevent leakage currents through the substrate during electrical measurements. The wafer was first cleaned with acetone and isopropanol in an ultrasonic bath for 5 minutes and then dried with nitrogen gas. In order to ensure the surface free of organic contaminants, oxygen plasma with low current (~5mA) was used to clean and etch the wafer surface before the deposition process.

The ferromagnetic layer (F2) (CoFe) of 50 μm thickness was deposited to form the upper layer of the SAF structure. This layer deposited at a current of 40 mA for 3 hours. The spacer layer (Ru) responsible of the antiferromagnetic coupling was deposited over the F2 layer with a thickness of 10 μm at current

 ISSN (print) 2958-8960 (online) 3006-6042 Printed in IRAQ

IRAQI JOURNAL OF MATERIALS
Volume (5) Issue (3) July-September 2026, pp. 121-126
Published and Sponsored by American Quality for Scientific Publishing, Inc. (AQSP)

of 35 mA for 2 hours. Ruthenium is a classical material to prepare SAFs as the strength and exchange highly depend on the spacer layer thickness due to the quantum oscillation effect. The ferromagnetic layer (F1) (CoFe) was deposited to form the lower layer of the SAF structure. This layer are similar to F2 layer in thickness (50 µm) and deposition parameters (current of 40 mA and deposition time of 3 hours). Both F1 and F2 layers should be identical by thickness and magnetic momentum in order to ideally satisfy the stray-field cancellation. CoFe alloy was selected due to its low damping factor and the possibility of vertical crystallization after thermal annealing, which facilitates the study of spin-orbit dynamics. A constant magnetic field of 500 Oe was applied along the substrate plane to determine the easy axis of the ferromagnetic layers. Platinum (Pt), tantalum (Ta), and tungsten (W) were selected as the heavy metal to deposit a layer with variable thickness (10-100 µm) on the F1 layer as the most important layer in this multilayer structure to induce the DMI as well as to generate the SOT. The layer thickness was controlled throughout varying deposition time considering a stable deposition rate of the magnetron sputtering system. Platinum shows relatively high deposition rate and can strongly and positively induce the DMI to generate specific chirality. A final thin layer of tantalum was deposited on the Pt layer to protect the magnetic layers from oxidation when exposed to the atmosphere.

Thermal annealing is an important step in the fabrication process of the proposed multilayer structure. It was carried out under vacuum at 350°C for one hour in inert environment of argon. Consequently, the amorphous CoFe layers convert into crystalline, which supports the perpendicular magnetic momentum as well as the magnetic resistance ratio [34,35].

The proposed experimental protocol to fabricate the multilayer structure represents the fundamental to prepare high-quality samples as it allows easily and reliably changing materials, thickness, and morphology.

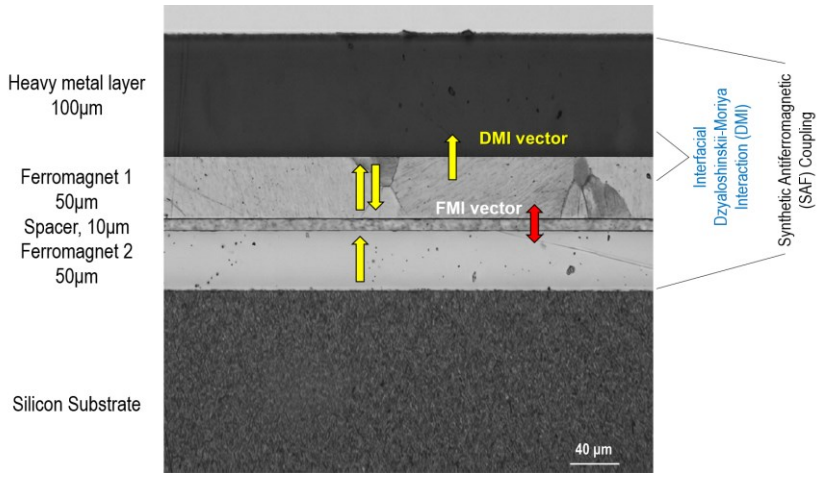

Fig. (1) Optical microscope image of the multilayer structure prepared in this work with labels showing layers and active regions

3. Results and Discussion

Figure (2) shows the variation of DMI energy density with the thickness of the heavy metal layer for three heavy metals used in this work. Platinum (Pt) layer showed the highest value of DMI with apparent peak when compared to the two other metals (Ta and W), which confirms its feature as a reference material for strong induced DMI that does not follow a linear or monotonic relationship with thickness of the heavy metal layer. A peak value of DMI (1.3 mJ/m^2) can be seen at 35 nm for Pt layer, 0.89 mJ/m^2 at 45 nm for Ta layer, and 0.7 mJ/m^2 at 45 nm for W layer. The sharp increase in DMI from 10 nm thickness to the peak value indicates an enhancement in the interface quality with increasing heavy metal layer thickness as the higher thickness allows the formation of a homogeneous crystalline structure with minimum defects that enhances the SOI [36].

Beyond the peak value, the DMI value decreases continuously with increasing layer thickness up to 75 µm as electrons lose their spin bonding before reaching the Pt/CoFe interface. As well, the crystal growth became less textured at larger thickness. As the layer thickness is further increased (80-100 µm), the DMI reached minimum and steady values of 0.7-0.73 mJ/m^2 for Pt, 0.48-0.58 mJ/m^2 for Ta,

 ISSN (print) 2958-8960 (online) 3006-6042 Printed in IRAQ

IRAQI JOURNAL OF MATERIALS
Volume (5) Issue (3) July-September 2026, pp. 121-126
Published and Sponsored by American Quality for Scientific Publishing, Inc. (AQSP)

and 0.3-0.35 mJ/m^2 for W. This result refers to the limited effect of the interface as the bulk contributions became dominant [37,38].

Tantalum shows the self-sharpening phenomenon as it can form an amorphous or nanocrystalline layer at very small thickness, which limits the DMI, whereas the decrease beyond the peak value may refer to higher electron dispersion in Ta layer than in Pt layer that may be attributed to its high electrical resistance. On the other hand, tungsten shows a reverse saturation behavior at larger thicknesses, which may explain that the W layer would suppress the DMI. This behavior may be attributed to different crystalline structures of tungsten phases (α-W and β-W) as the β-W shows higher stability at smaller layer thickness and hence enhances SOI much better than the α-W dominating at larger layer thickness [39-42]. Accordingly, the phase transformation from β-W to α-W with increasing layer thickness may explain the sharp decrease in DMI.

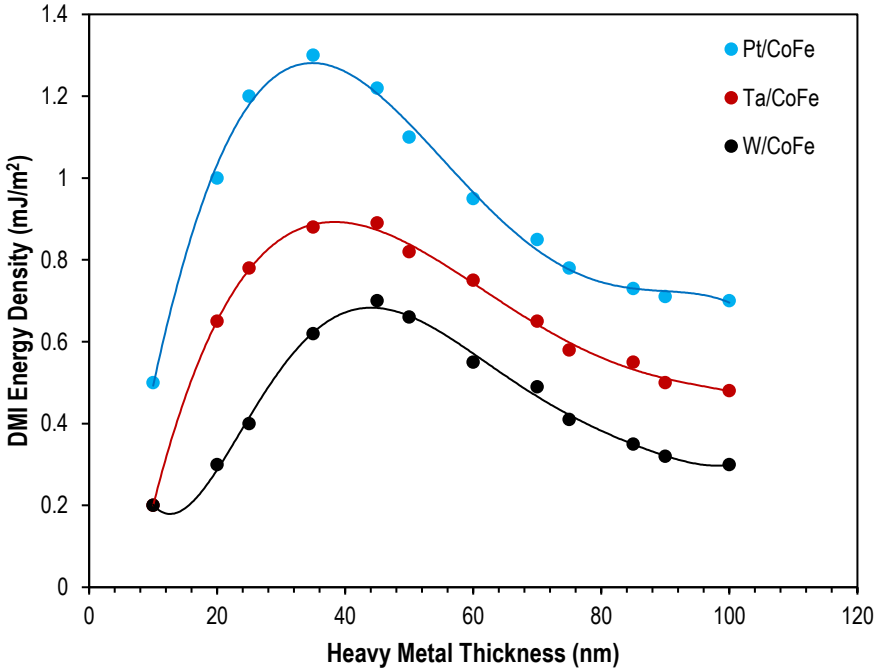

Fig. (2) Interfacial Dzyaloshinskii-Moriya Interaction (DMI) versus heavy metal layer thickness for three different heavy materials

Figure (5) shows the variation of the domain wall velocity with current density for the Pt/FM1/SPACER/FM2/Si structure as optimized model compared to standard model. It is clear that the optimized model is apparently superior as the domain wall began to move at very low current density threshold of 1.2x10^{11} A/m^2 whereas the standard model required higher current density to start the movement. The optimized model achieved ultrafast velocities (~10^3 m/s) while the standard model showed steady (or saturated) velocity not exceeding 400 m/s. This indicates the efficient physical modifications in the optimized model that reduced the friction forces or internal obstacles and hence allowed faster and much more efficient dynamic responses. This is very crucial to develop the memories of the advanced computers and spintronics [43-45].

4. Conclusion

In conclusions, platinum was found the optimum to achieve the highest DMI energy density of 1.3 mJ/m^2 at platinum layer thickness of 35 μm while the performance was decreased when tantalum or tungsten were used. Also, the domain wall velocity was semi-linearly increasing with current density to reach a saturation at 6x10^{11} A/m^2 due to the Walker breakdown phenomenon. The most interesting result was observed by the optimized model of the multilayer structure proposed in this study that achieve ultrahigh velocity of 10^3 m/s at low threshold current density (1.2x10^{11} A/m^2) with superiority over the standard model. These results reveal the possibility to accurately design the spin chirality throughout the enhancement of the heavy metal layer leading to drastic development in ultrafast and low-energy spintronics.

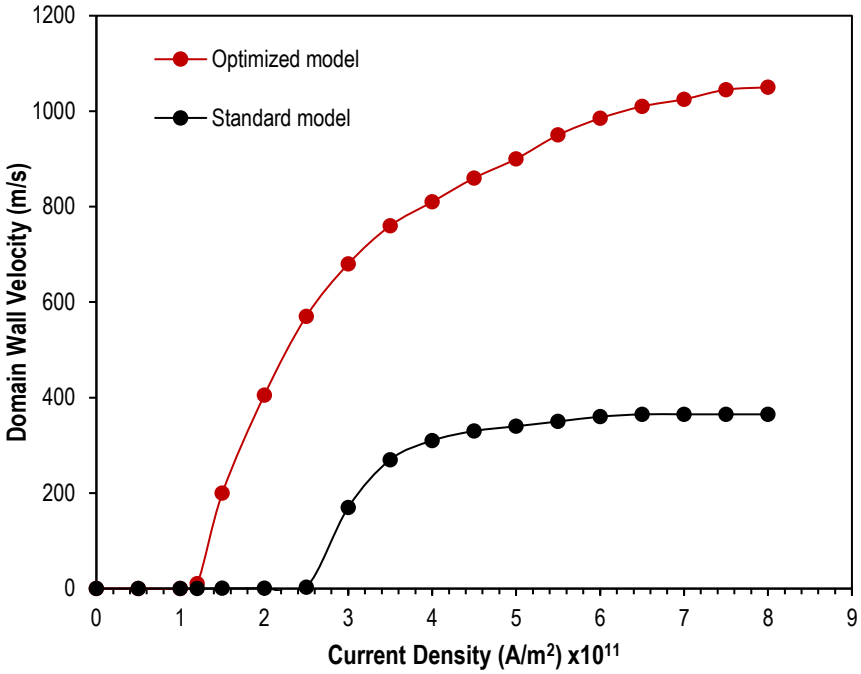

Fig. (5) Variation of the domain wall velocity with the current density for the Pt/FM1/SPACER/FM2/Si structure as optimized model compared to standard model

References

[1] S. Ning et al., "Challenges and opportunities for spintronics based on spin orbit torque", Fundament. Res., 2(4) (2022) 535-538.
[2] G. Zhang et al., "Progress and challenges for two-dimensional spin-polarized quantum materials", Cell Rep. Phys. Sci., 6(1) (2025) 102356.
[3] J. Qiu et al., "Raman study of the spin–lattice excitations of the layered antiferromagnets $MPSe_3$ (M = Fe, Mn)", Result. Phys., 56 (2024) 107256.
[4] P. Liu et al., "Recent advances in 2D van der Waals magnets: Detection, modulation, and applications", iScience, 26(9) (2023) 107584.
[5] Z. Wang et al., "Field-free spin-orbit torque switching of synthetic antiferromagnet through interlayer Dzyaloshinskii-Moriya interactions", Cell Rep. Phys. Sci., 4(4) (2023).
[6] A. Hirohata et al., "Characteristic frequencies in magnetic and spintronic phenomena", Newton, 1(7) (2025) 100192.
[7] A. Hoffmann, "A personal spin on spin currents", J. Magn. Magnet. Mater., 645 (2026) 173979.
[8] G. van der Laan and T. Hesjedal, "X-ray detected ferromagnetic resonance techniques for the study of magnetization dynamics", Nucl. Instrum. Meth. Phys. Res. B: Beam Interact. Mater. Atoms, 540 (2023) 85-93.
[9] X. Jiang et al., "Two-dimensional MXenes: From morphological to optical, electric, and magnetic properties and applications", Phys. Rep., 848 (2020) 1-58.
[10] S. Shi et al., "Recent progress in strong spin-orbit coupling van der Waals materials and their heterostructures for spintronic applications", Mater. Today Electron., 6 (2023) 100060.
[11] R.E. Camley and K.L. Livesey, "Consequences of the Dzyaloshinskii-Moriya interaction", Surf. Sci. Rep., 78(3) (2023) 100605.
[12] V. Tsurkan et al., "On the complexity of spinels: Magnetic, electronic, and polar ground states", Phys. Rep., 926 (2021) 1-86.
[13] M.L. Kulić, "Conventional magnetic superconductors: coexistence of singlet superconductivity and magnetic order", Comptes Rendus Physique, 7(1) (2006) 4-21.
[14] D.A. Carvajal, A. Riveros, and J. Escrig, "Orbit-like trajectory of the vortex core in ferrimagnetic dots close to the compensation point", Result. Phys., 19 (2020) 103598.
[15] P. Chen, H. Chi, and J.S. Moodera, "Progress and prospects of magnetic topological materials for spintronic applications", Newton, (2026) 100436.
[16] M. Coll et al., "Towards Oxide Electronics: a Roadmap", Appl. Surf. Sci., 482 (2019) 1-93.
[17] M. Jazandari, J. Abouie, and D. Vashaee, "Unifying thermopower: entropy and specific heat in magnetic, superconducting, nanoscale, and frustrated systems", iScience, 29(2) (2026) 114565.
[18] S.N. Datta, A.K. Pal, and A. Panda, "Design of magnetic organic molecules and organic magnets: Experiment, theory and computation with application and recent advances", Chem. Phys. Impact, 7 (2023) 100379.
[19] J. Han et al., "Unconventional responses in non-collinear antiferromagnets", Newton, 1(1) (2025) 100012.
[20] S. Husain, Z. Yao, and R. Ramesh, "Enabling magnetoelectric spin-orbit logic and memory", Newton, 1(1) (2025) 100026.
[21] Y. Ma et al., "Ultrafast and reliable domain-wall and skyrmion logic in a chirally coupled ferrimagnet", Newton, 1(9) (2025) 100208.
[22] D. Xiong et al., "Antiferromagnetic spintronics: An overview and outlook", Fundament. Res., 2(4) (2022) 522-534.

[23] B. Wu et al., "Electrically manipulating exchange bias and realizing multiple remanent states in platinum/cobalt/iridium manganese heterostructures", Cell Rep. Phys. Sci., 5(1) (2024) 101757.
[24] J. Gracia, "Quantum catalysts", EES Catal., 3(5) (2025) 994-1029.
[25] D. Bang, P.V. Thach, and H. Awano, "Current-induced domain wall motion in antiferromagnetically coupled structures: Fundamentals and applications", J. Sci.: Adv. Mater. Dev., 3(4) (2018) 389-398.
[26] C. Tang et al., "Spin dynamics in van der Waals magnetic systems", Phys. Rep., 1032 (2023) 1-36.
[27] B. Göbel, I. Mertig, and O.A. Tretiakov, "Beyond skyrmions: Review and perspectives of alternative magnetic quasiparticles", Phys. Rep., 895 (2021) 1-28.
[28] G.M. Kanyolo et al., "Honeycomb layered frameworks with metallophilic bilayers", Prog. Mater. Sci., 141 (2024) 101205.
[29] H.Y. Yuan et al., "Quantum magnonics: When magnon spintronics meets quantum information science", Phys. Rep., 965 (2022).
[30] O.A. Hammadi, W.N. Raja, M.A. Saleh and W.A. Altun, "Magnetic Field Distribution of Closed-Field Unbalanced Dual Magnetrons Employed in Plasma Sputtering Systems", Iraqi J. Appl. Phys., 12(3) (2016) 35-42.
[31] O.A. Hammadi, M.K. Khalaf, F.J. Kadhim and B.T. Chiad, "Operation Characteristics of a Closed-Field Unbalanced Dual-Magnetrons Plasma Sputtering System", Bulg. J. Phys., 41(1) (2014) 24-33.
[32] O.A. Hammadi, M.K. Khalaf and F.J. Kadhim, "Fabrication of UV Photodetector from Nickel Oxide Nanoparticles Deposited on Silicon Substrate by Closed-Field Unbalanced Dual Magnetron Sputtering Techniques", Opt. Quantum Electron., 47(12) (2015) 3805-3813.
[33] A.M. Hameed and M.A. Hameed, "Highly-Pure Nanostructured Metal Oxide Multilayer Structure Prepared by DC Reactive Magnetron Sputtering Technique", Iraqi J. Appl. Phys., 18(4) (2022) 9-14.
[34] M. Mohylna, V. Tkachenko, and M. Žukovič, "Towards skyrmion crystal stabilization in the antiferromagnetic triangular lattice at ambient conditions", Phys. Lett. A, 490 (2023) 129170.
[35] N. Ghobadi, R. Daqiq, and S.A.H. Moradi, "Improved tunnel magnetoresistance by double-barrier magnetic tunnel junctions with a layered antiferromagnet material", Result. Phys., 70 (2025) 108171.
[36] X.C. Hu et al., "Recent progress in magnetic skyrmion morphology", Rev. Phys., 13 (2025) 100111.
[37] Z. Lei et al., "Manipulation of ferromagnetism in intrinsic two-dimensional magnetic and nonmagnetic materials", Matter, 5(12) (2022) 4212-4273.
[38] K.H. Andersen et al., "The instrument suite of the European Spallation Source", Nucl. Instrum. Meth. Phys. Res. A: Accel. Spectrom. Detect. Assoc. Equip., 957 (2020) 163402.
[39] G. Tatara, "Effective gauge field theory of spintronics", Physica E: Low-dimen. Syst. Nanostruct., 106 (2019) 208-238.
[40] Z. Dai et al., "Magnetic field driven emergent phenomena: Insights from magneto-optics and nanoscopy", Prog. Quant. Electron., 103 (2025) 100585.
[41] I. Žutić et al., "Proximitized materials", Mater. Today, 22 (2019) 85-107.
[42] Y. Yang et al., "Strain effects on multiferroic $BiFeO_3$ films", Comptes Rendus Physique, 16(2) (2015) 193-203.
[43] S.-B. Zhang et al., "Spin-valley locking and pure spin-triplet superconductivity in noncollinear antiferromagnets proximitized to conventional superconductors", Newton, (2026) 100379.
[44] A. Brataas et al., "Spin insulatronics", Phys. Rep., 885 (2020) 1-27.
[45] Y. Cao et al., "Prospect of Spin-Orbitronic Devices and Their Applications", iScience, 23(10) (2020) 101614.
[46] J. Maggiora, X. Wang, and R. Zheng, "Superconductivity and interfaces", Phys. Rep., 1076 (2024) 1-49.
[47] S. Sarkar et al., "Spin band geometry drives thermal spin magnetization and current", Mater. Today Quantum, 10 (2026) 100062.
[48] T. Nie et al., "Two-dimensional ferromagnetic materials: Enabling next-generation spintronics at the nanoscale", Rev. Mater. Res., 2(1) (2026) 100145.
[49] Y. Wei, H. Liu, and K. Wang, "Magnetic anisotropy and phononic properties of two-dimensional ferromagnetic Fe_3GeS_2 monolayer", iScience, 27(9) (2024) 110781.

 ISSN (print) 2958-8960 (online) 3006-6042 Printed in IRAQ